Spectral analysis of a ghost

Nasser S. Hamarbatan and Gary F. Margrave

ABSTRACT

The vertical component of the Blackfoot high-resolution of 3C-2D data from two different source patterns was processed and two different stacks were produced. One source pattern consisted of 4 kg of explosives in a single 18 m hole. The second pattern consisted of 2 kg of explosives in each of two 9 m holes. A dramatic difference between the migrated stacks of the two datasets was observed. An f-x analysis was run to display the amplitude and phase spectra of the unmigrated datasets. Similar analysis was run on representative shot gathers from the two datasets. The analysis shows that the 9 m data has a higher signal band than the 18 m data has. A spectral notch due to a surface source ghost reflection is suggested as the main cause of the lower signal band in the 18 m dataset. A frequency of 55 HZ for the spectral notch was interpreted from various spectra. Further processing and analysis were run to confirm the estimated frequency. Due to the spectral notch in the 18 m data, better resolution was observed in the 9 m stacks than in the 18 m stacks. A theoretical ghost operator which installs a notch at the mentioned frequency was convolved with a 9 m migrated trace and compared to corresponding migrated traces from the 18 m data. A match between the resulting traces was observed.

INTRODUCTION

The CREWES project at the University of Calgary conducted a high-resolution 3C-2D seismic survey at Blackfoot field in November 1997. The Blackfoot field is located southeast of the town of Strathmore, Alberta.

The 3 km 3C-2D line consisted of a combination of normal and high resolution receiver intervals. The source interval for the entire line was 20 m. There were a total of 151 shot points of 4 kg charge size loaded in a single hole at 18 m depth and positioned on the half station. The receiver interval for the 1st and 3rd km of the recording spread was 20 m. This gave a total of 50 3-C geophones for each km. In the central high-resolution km, the receiver interval was 2 m making a total of 501 3-C geophones for the center km of the spread. This would give a total of 601 3-C geophones planted along the 3 km line. All the geophones were buried at a depth of about 50 cm to eliminate wind noise. See Stewart et al. (1997) for further description and initial results.

To test the effect of the source depth on the resolution of the data, an additional 15 shot points were added at the center of the line which consisted of 2 holes at 9 m depth loaded with a 2 kg charge in each hole. These extra 2-hole patterns were drilled close to corresponding single hole shots such that both an 18m-hole and a 9m-hole have the same shotpoint number. This allowed the creation of an 18 m data (a subset of the total line) which has only 15 shots that compared directly to the 9 m dataset. Figure (1) shows a sketch of the field layout for the Blackfoot survey for the central high-resolution kilometer.

In both unmigrated and migrated data, a difference between the 9 m and 18 m datasets was noticed. An f-x analysis (Margrave, 1995 and 1999) of both unmigrated datasets was run to compare them in terms of their signal bandwidth and their amplitude

as a function of frequency. Further analyses of both raw and migrated datasets were also run to confirm the observed differences.

In this paper the processing steps, which were applied to both datasets, will be discussed and unmigrated and migrated sections will be shown. Displays of the f-x analysis along with the average amplitude spectra of the unmigrated datasets will also be presented and show a difference in both frequency content and signal power. The amplitude spectra of some selected windows from the raw of 18 m and 9 m data were computed and show a difference between the shot gathers with respect to their maximum amplitudes. The difference between the datasets is suggested as due to a spectral notch in the 18 m data caused by a surface source ghost reflection. The theory of the ghost and the notch are also discussed.

DATA PROCESSING

Using ProMAX software, both 18 m and 9 m raw datasets were processed and two different sections were produced. Figure (2) shows a flowchart of the processing steps which were followed to process both datasets. The static corrections including residual statics were computed separately for each dataset. Prestack TVSW (Time Variant Spectral Whitening) (Yilmaz, 1987) of 5 to 90 HZ was one of the tools applied in the processing scheme and spectra analysis was done on the resultant stack. The same analysis was run after a poststack TVSW of 5 to 90 HZ. To minimize the influence of the ground role, care was taken to chose a decon operator design gate such that it omits the middle part of the shot gather where the ground role is strong, especially in the 9 m data. The f-x decon was applied to the poststack TVSW section before phase shift migration.

The unmigrated stacked sections are shown in figures 3 and 4. The 9 m dataset is referred as 2 x 9 m in all the displays while the 18 m data referred as 1 x 18 m to indicate the number of holes at each shotpoint. Figure 3 shows the unmigrated stack of both 18 m data (top) and 9 m data (bottom) with a selection window which was chosen for an enlarged display. The selection window covers from CDP 1592 to CDP 1800 and from 500 ms to 1200 ms. Figure 4 shows the enlargements for both unmigrated datasets in the selection windows.

The migrated sections of both 18 m and 9 m data are shown in figure 5. A window having the same dimensions as the one in the unmigrated data was selected for enlarged display. A better assessment of the difference between the two sections could be made after migration. The difference is clear in the zoomed windows in figure 6 which shows each selection window from each section divided vertically into left and right parts. Each part from one dataset was plotted next to the same part from the other data. In this figure, the difference between the two datasets is clearly observed. For example, in the section between 900 ms and 1200 ms there is better temporal resolution and more events appear in the 9 m data than were in the 18 m data. In the shallower part of both windows there are more coherent signals in the 9 m data than are in the corresponding section of 18 m data.

ANALYSES AND OBSERVATIONS

The unmigrated data sets were transferred to Matlab for f-x analysis and amplitude spectra computations. The entire sections for both 18 m and 9 m data, record length of 2 seconds, were used in the analysis. The f-x amplitude spectra, complex phase spectra and the average amplitude spectra were computed for each dataset. The prestack TVSW stack was first analyzed and some observations are discussed below.

Contents

Figure 7 shows the f-x amplitude spectra of prestack TVSW stack for both 18 m and 9 m data. The maximum power of the signals, which is full black, indicates the frequency band over which the stacked section has good spectral power (Margrave,1995) . In the 18 m spectrum, there is good spectral power in a frequency band from 10 to 50 HZ, while the 9 m stacked section has spectral power up to 60 HZ. Signal can also be identified by lateral frequency coherence which is probably controlled by the near surface geology. It is suggested that the limited spectral power in the 18 m spectrum is due to a spectral notch at a frequency of 55 HZ resulting from a source ghost reflection off of the recording surface .

Figure 8 shows the complex phase spectra of prestack TVSW stack for the 18 m and 9 m data. In this figure there is also evidence of a spectral notch in the 18 m data which is represented by incoherent phase above 50 HZ. The 9 m phase spectrum shows coherence almost up to 65 HZ and in some locations there is signal near 70 HZ.

The average amplitude spectra for the mentioned datasets were computed and are shown in figure 9. The average amplitude spectra for 18 m and 9 m data are shown in figures 9a and 9b respectively. For a better comparison, figure 9 (c) superimposes both amplitude spectra. It can be seen that both amplitude spectra are nearly identical up to 50 HZ. Since this data had TVSW applied immediately before stack, the spectrum of the unstacked data was white out to 90 HZ. The extent to which it has “unwhitened” in stacking is shown in these average amplitude spectra. Since both datasets are noise dominated at 90 HZ, the average amplitude spectra level at 90 HZ can be taken as an indicator of pure noise. Comparing the 9 m and 18 m data in the 50 to 60 HZ region shows that the 18 m data has stacked like noise while the 9 m has stacked like signal

As the non-source related acquisition parameters and the processing were identical for both datasets, it is suggested that the lower resolution in the 18 m dataset and the higher resolution in the 9 m dataset is governed by the frequency of a spectral notch which is a function of the source depth. Different processing tools and further analyses were run on both datasets to investigate this in more detail.

TVSW was applied to the stacked datasets to enhance the amplitude of all the frequencies. The purpose of this test is to demonstrate that spectrally whitening the 18 m dataset will not make it equivalent to the 9 m data. Figure 10 shows the f-x amplitude spectra of poststack TVSW for 18 m and 9 m data and the elevation changes along the line. Although the amplitude of the spectrum is boosted, coherence is still limited to 50 HZ in the 18 m spectrum and to 65 HZ in the 9 m spectrum. Spectral whitening has enhanced all the frequencies including noise, but the coherency kept its characteristics at the mentioned frequencies in both datasets.

The phase spectra of the poststack TVSW (figure 11) showed similar results to the prestack TVSW phase spectra (figure 8). This indicates that some of the whitened frequencies were noise. Although the noise was whitened along with the signal, it still lacks phase coherence. Figure 12 shows the effect of the whitening in more detail. The average amplitude spectrum of 18 m data (figure 12a) shows that all the frequencies in the spectrum were whitened to almost the same level. The same case for the 9 m data is illustrated in figure 12b. Both figures were superimposed to show the correlation between the two spectra (figure 12c). As it was shown in figure 9c, the difference between the two spectra was within the frequencies 50 to 65 HZ. The same difference is preserved in the poststack TVSW spectra. Similarly the amplitude spectra for both datasets are nearly identical up to 50 HZ. This remarkable result indicates that the difference between the 18 m and 9 m data above 50 HZ is not due to artifacts caused by

the processing parameters or any effects (such as geology) other than to a frequency notch in the 18 m data as a result of a source ghost reflection.

GHOST THEORY

When a buried source is detonated the waves will travel in all directions and some of the waves will reflect at the surface and travel back into the earth causing what is called a source ghost. The energy traveling downward from the source is superimposed upon the ghost energy (Sheriff and Geldart 1995). By the time the reflected wave (ghost) returns to the source point it has traveled a time $t_g = \frac{2\Delta Z}{V_W}$ where ΔZ is the source depth and V_W is the weathering velocity. This ghost will cause a spectral notch in the recorded data at a frequency $f_g = \frac{1}{t_g}$, then from the definition of t_g, the notch frequency $f_g = \frac{V_W}{2\Delta Z}$ (Hatton et al. 1986).

Both the weathering velocity and the source depth have an effect in defining the notch frequency. For very shallow sources the weathering velocity usually has little change with depth so the main factor in defining the notch frequency will be the depth. It can be concluded that the deeper the source the lower the notch frequency. If the notch occurs, it is more likely that its frequency will be within the signal band of the data. As the source is placed deeper in the ground the notch frequency moves to the lower part of the spectrum and more signals will be hurt and lower resolution will be the result. To avoid the notch in the signal band, a shallower source should be considered. Given a higher notch frequency, it is more likely that it will fall out of the signal band of the data and better resolution will be obtained.

From Figure 13 it can be seen that the notch will degrade signals in a significant bandwidth around the central frequency. Although the central frequency of the notch was suggested as 55 HZ in the 18 m data, some more signal with higher and lower frequencies than 55 HZ were also degraded. Some signal above 65 HZ is evident in the 18 m data (figures 7 and 8 top) where a maximum coherent frequency near 80 HZ could be observed. The 9 m spectra analysis showed coherence frequency from 10 to 65 HZ. This suggests that there may be a spectral notch at higher frequency causing signal disappearance above 65 HZ. As the source depth decreases, the frequency at which the spectral notch occur will be higher (Hatton at al. 1986).

The possibility of a source ghost in the Blackfoot data has been mentioned previously by Margrave (1995). Figure 14 is taken from the Blackfoot Broadband survey, shot in 1995, which also used a single hole at 18 m source configuration. A spectral notch is evident on both the amplitude and phase spectra as zones of low power and low coherence near 55 HZ. The notch correlates spatially with topography of the line.

FURTHER ANALYSES

As mentioned previously for figures 9c and 12c, the amplitude spectra for both datasets are nearly identical up to 50 HZ. Another way to confirm this identity was to apply a bandpass filter of 0 to 50 HZ to both migrated stacks of 18 m and 9 m data. The resultant stacks are shown in figure 15 and are very similar in terms of coherency, number of events and time matching.

Contents

Two raw shot gathers from 18 m and 9 m data were exported to Matlab for average amplitude spectra computations. Three different windows were selected in each shot gather (Figure 16). The first window was selected such that part of the refracted signals from each shot gather would be analyzed. The second window covers a large part of the ground roll in each gather and the third selection window was designed such that the reflected signal in the far offset would be analyzed.

Figure 17a shows the superimposed average amplitude spectra of each shot gather in window #1. The 18 m refracted signals have more power than the 9 m signal. This may be because the distance from the source to a refractor and then to the surface is shorter for the 18 m signals than for 9 m signals. Figure 17b shows the same spectra with a decibel scale with respect to the maximum amplitude of the 18 m data.

The average amplitude spectra of window #2 from each shot gather were computed and superimposed and are shown in Figure 18a. As expected, the ground roll for the 9 m shot gather has more power than the 18 m. This is a disadvantage of using a shallow source pattern which can be treated in the processing if the recording system has sufficient dynamic range. Figure 18b shows both average amplitude spectra with a decibel scale with respect to the maximum amplitude of the 9 m data.

Window #3 from each shot gather was analyzed and the average amplitude spectra were computed. Figure 19a shows both spectra superimposed and suggests similar power of the reflected signal for both shots. Figure 19b is a decibel display of the average amplitude spectra for the same window and shows a difference between the 9 m and 18 m data from 55 to 70 HZ. This probably related to the same difference in the processed data when the amplitude spectra in figures 9c and 12c were nearly identical up to 55 HZ.

It has been suggested that a spectral notch due to a surface source ghost reflection is the main cause of the lower signal band in the 18 m dataset. The frequency of the notch was interpreted as a result of the spectral analysis of both 18 m and 9 m datasets and was estimated as 55 HZ. A theoretical ghost operator which installs a notch at the mentioned frequency was then convolved with a 9m-migrated trace and compared to corresponding migrated traces from the 18 m data (figure 20). A match between the resulting traces was observed at a time window from 700 to 1200 ms. Figure 21 is a similar display to figure 20 except that normal a 9m migrated trace is compared to corresponding migrated traces from 18 m data and shows a mismatch between the two different traces in terms of time, frequency and amplitude.

CONCLUSIONS

Combining the information from the f-x analysis of the 18 m and 9 m data, it can be stated that in the Blackfoot high-resolution 3C-2D survey reflection signal band starts at 5 HZ and extend up to 80 HZ. Lower resolution on the 18 m data was encountered as a result of a spectral notch at 55 HZ caused by a source ghost reflection and a similar spectral notch is postulated for the 9 m data at a frequency above 70 HZ. Both weathering velocity and source depth determine the notch frequency. These two factors should be considered in designing the source pattern in the field. It can also be concluded that the f-x analysis is a good estimator of the recorded signal band of raw data as well as unmigrated sections. As a result of these analyses a source depth of 9 m or less is suggested for any future Blackfoot survey.

ACKNOWLEDGMENTS

We would like to thank Brian Hoffe and Henry Bland for their help during this process. Also we would like to thank the CREWES Project Sponsors for their financial support.

REFERENCES

Hatton, L, Worthington, M., Makin, J, 1986, Seismic Data Processing - Theory and Practice: Blackwell Scientific Publications.

Margrave, G. F., 1999, Seismic signal band estimation using f-x spectra: Geophysics, in press (to appear Jan. - Feb. 1999).

Margrave, G. F.,1995, Estimates of the signal band of the Blackfoot broad-band data, CREWES Research Report, Volume 7.

Stewart, R., Hoffe, B., Bland, H., Margrave, G., Gallant, E., and Bertram, M., 1997, The Blackfoot high resolution 3-C Seismic survey: Design and initial results, CREWES Research Report, Volume 9.

Sheriff, R., and Geldart, L.,1995, Exploration Seismology, Second edition. Press Syndicate of the University of Cambridge.

Yilmaz, O., 1987, Seismic data processing. Society of Exploration Geophysics.

Hatton, L, Worthington, M., Makin, J, 1986, Seismic Data Processing - Theory and Practice: Blackwell Scientific Publications.

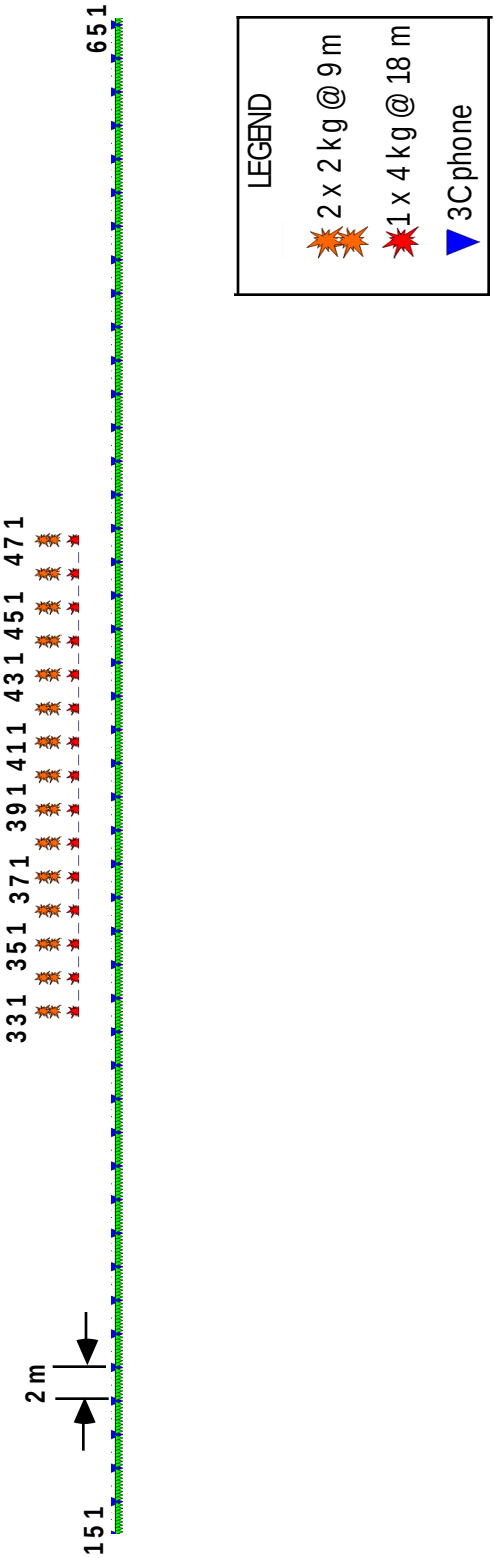

FIGURE 1. A sketch of the field layout for the high resolution part.

Contents

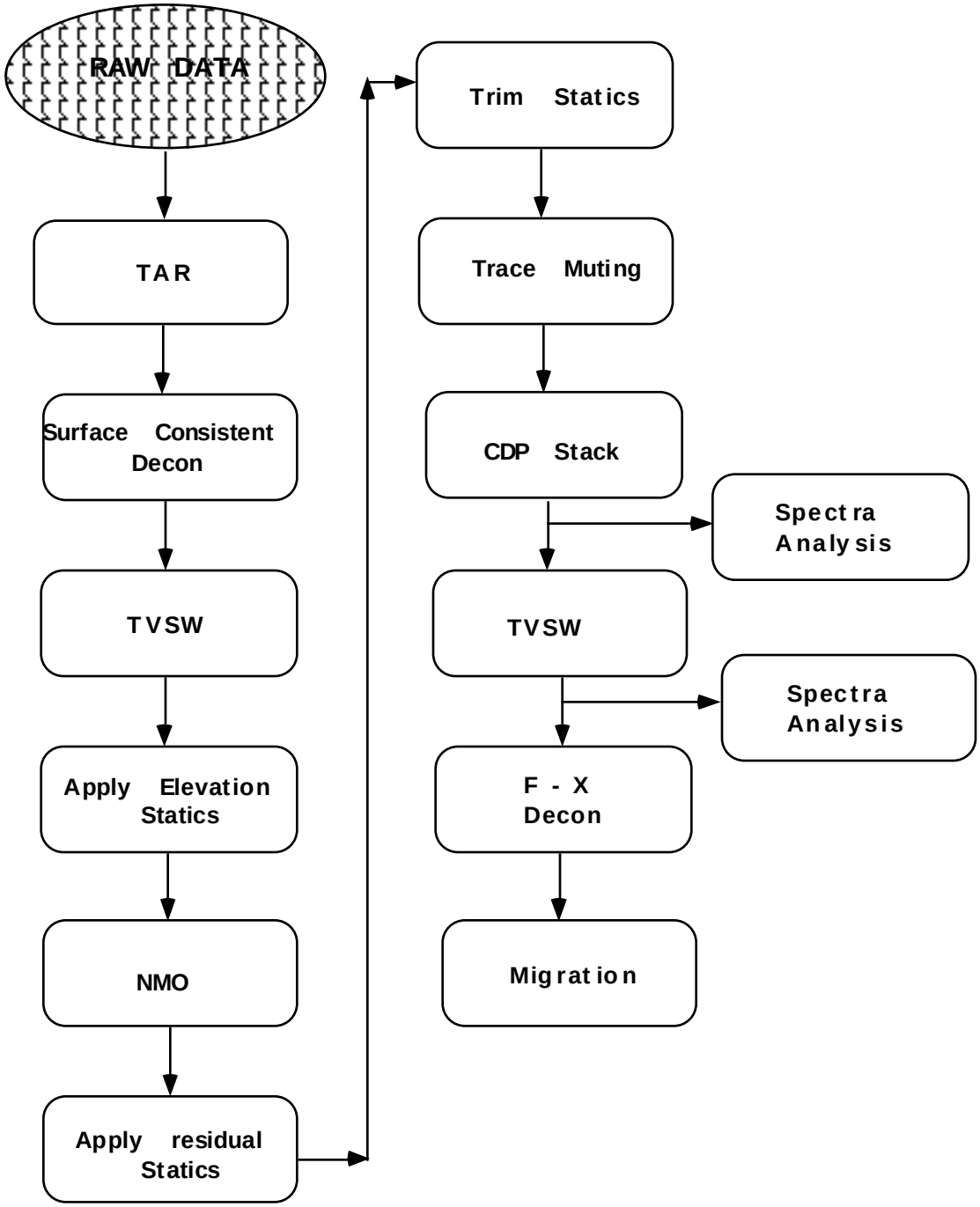

FIGURE 2. The flowchart of the processing steps applied.

Contents

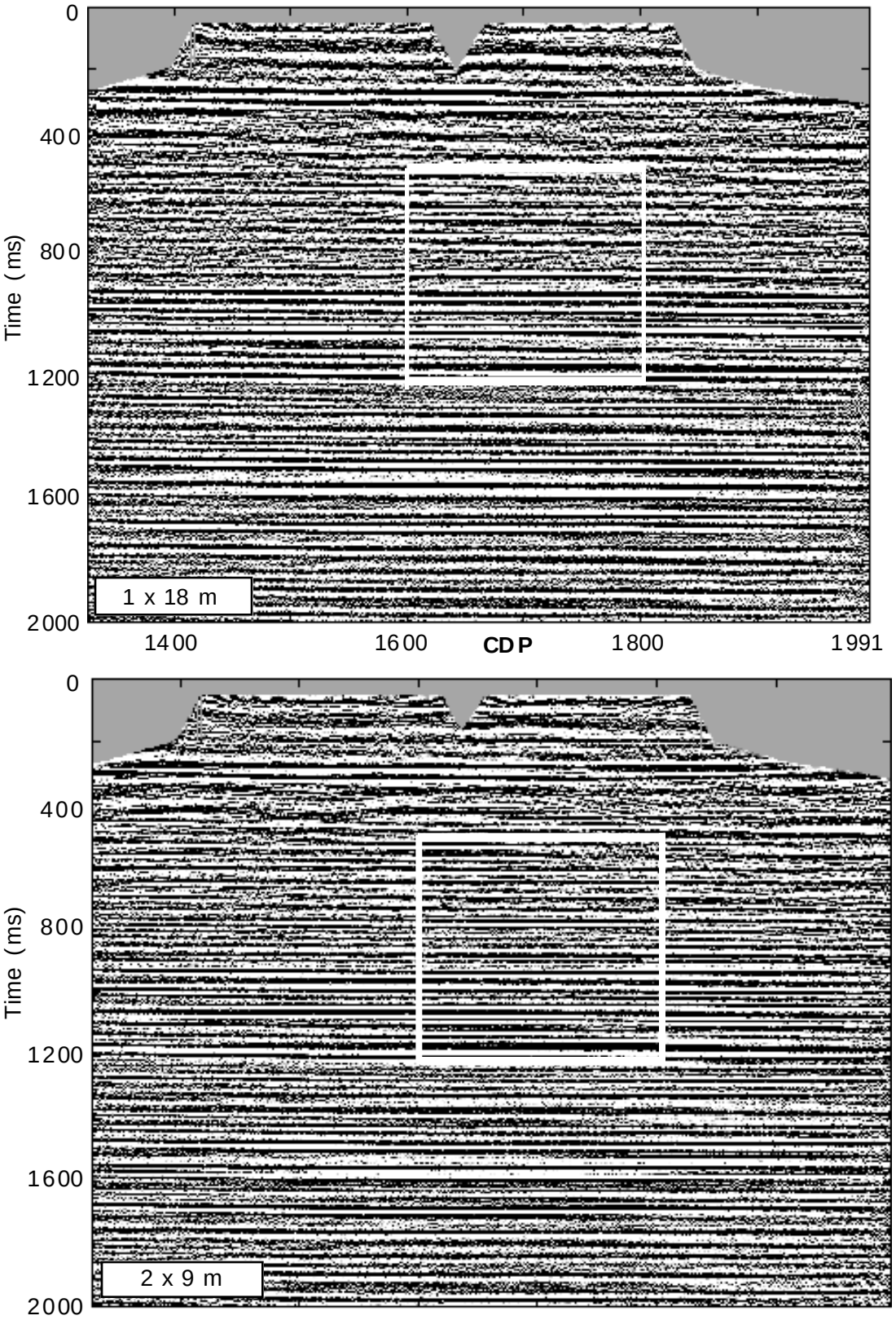

FIGURE 3. Unmigrated prestack TVSW stacks of 18 m and 9 m data sets with selection windows shown in Figure 4.

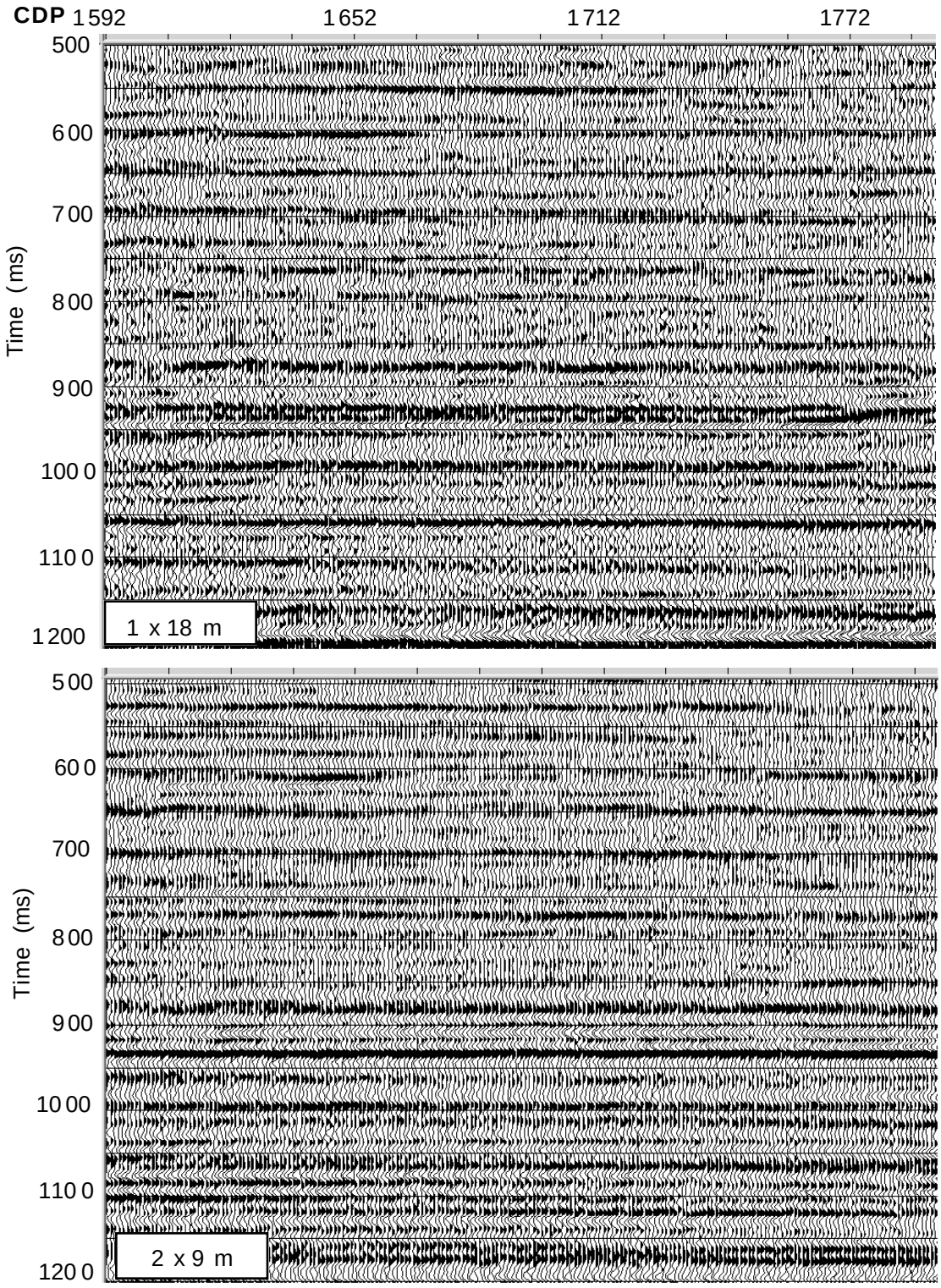

FIGURE 4. Both selection windows from the unmigrated 18 m and 9 m data in Figure(3).

Contents

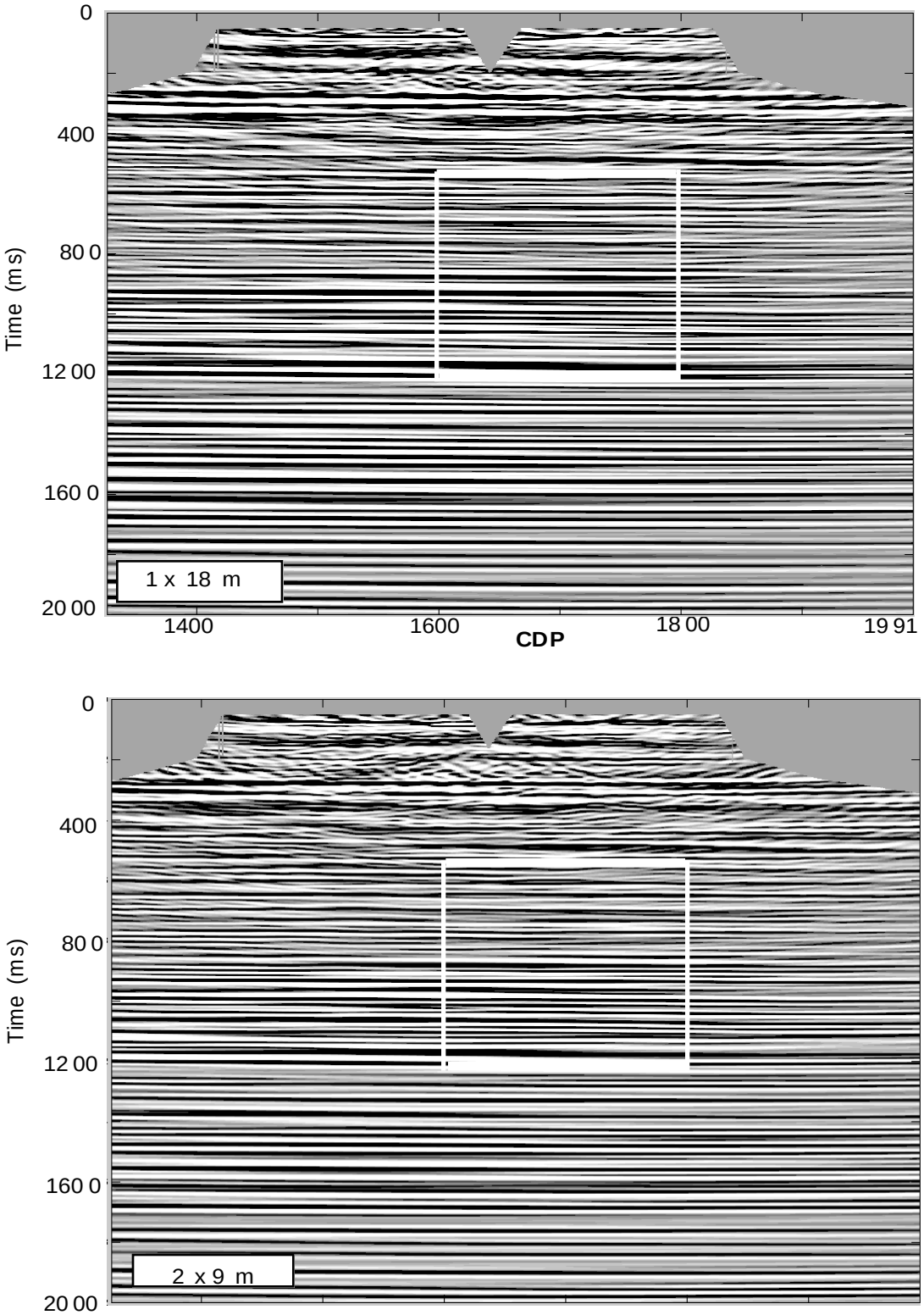

FIGURE 5. The migrated prestack whitening stacks of 18 m and 9 m data sets with selection windows shown in Figure 6.

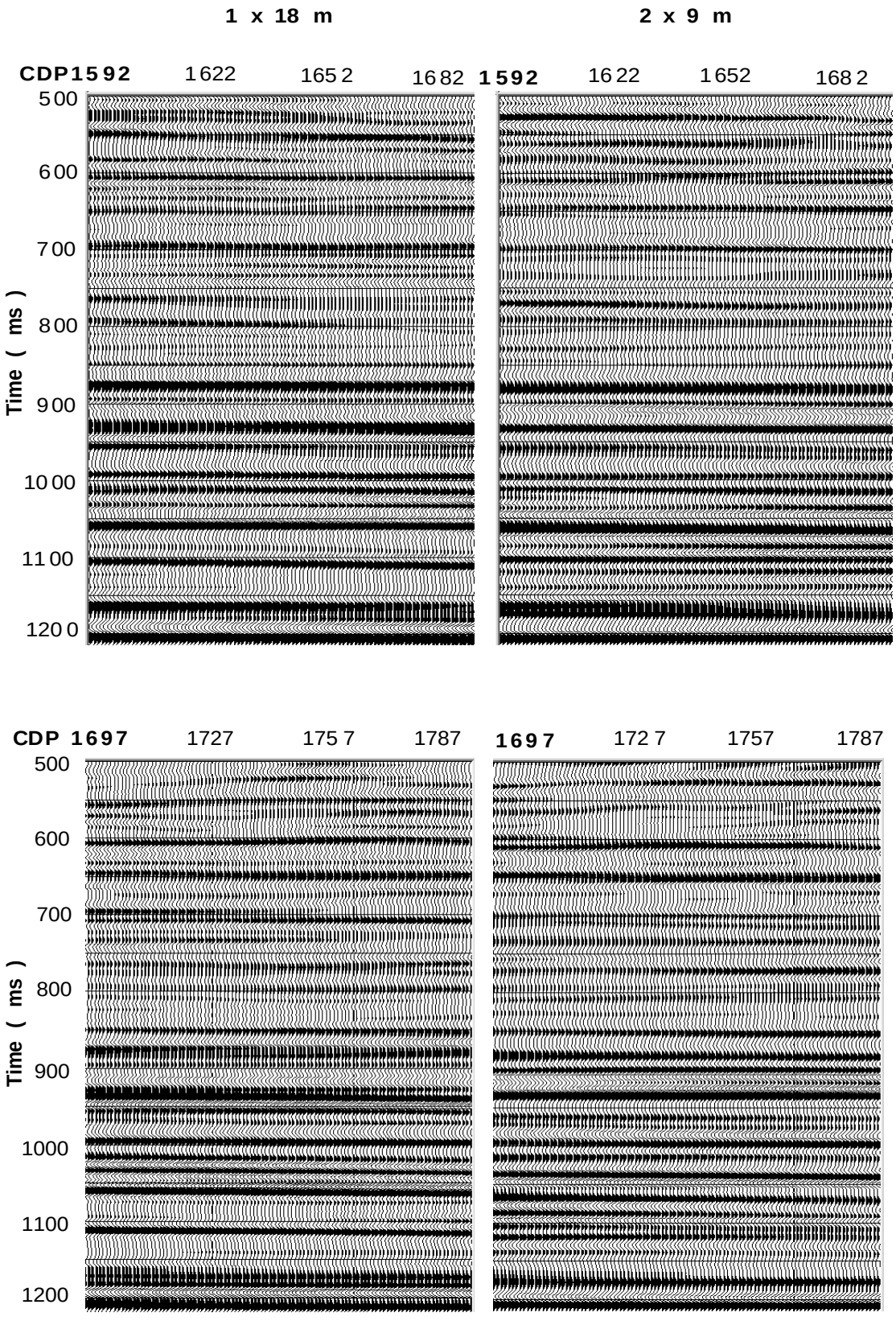

FIGURE 6. Two parts of the selection windows from the migrated 18 m and 9 m data in Figure 5. On top are the left halves of the windows while on bottom are the right halves

Contents

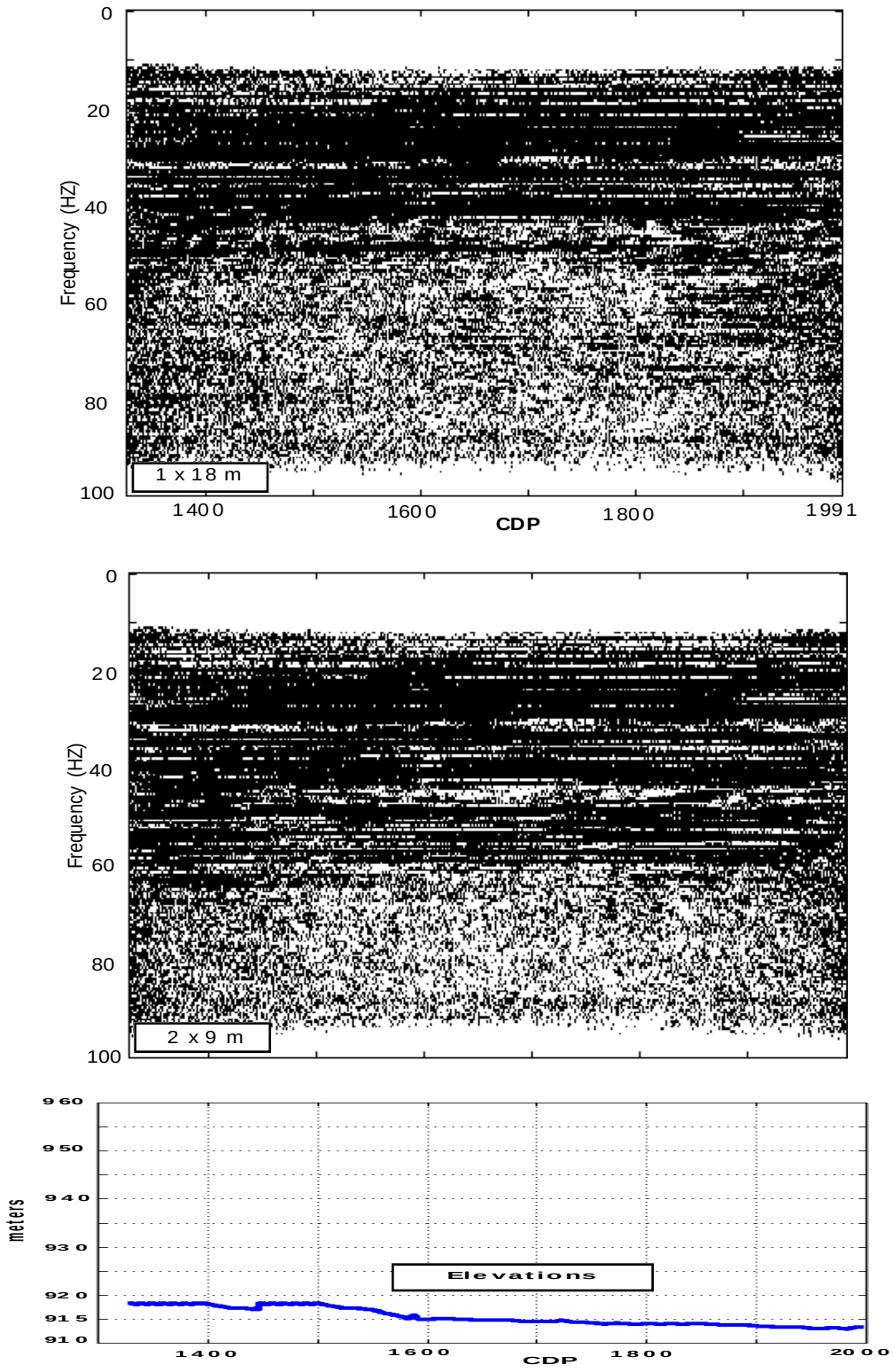

FIGURE 7. The f-x amplitude spectra of the unmigrated prestack TVSW of 18 m and 9 m data and the elevation changes along the processed line.

Contents

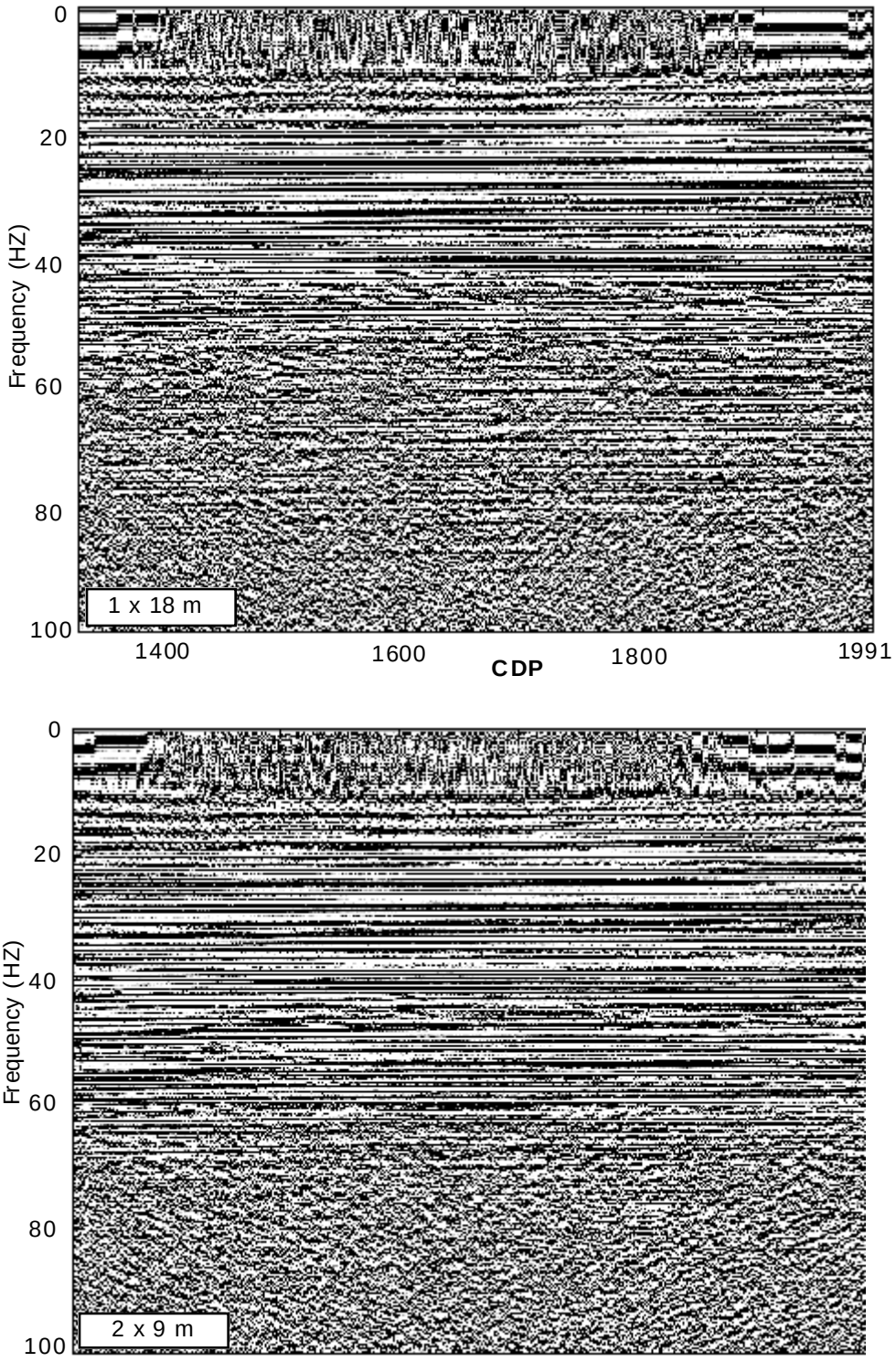

FIGURE 8. The f-x phase spectra of the unmigrated prestack TVSW of the 18 m and 9 m data

Contents

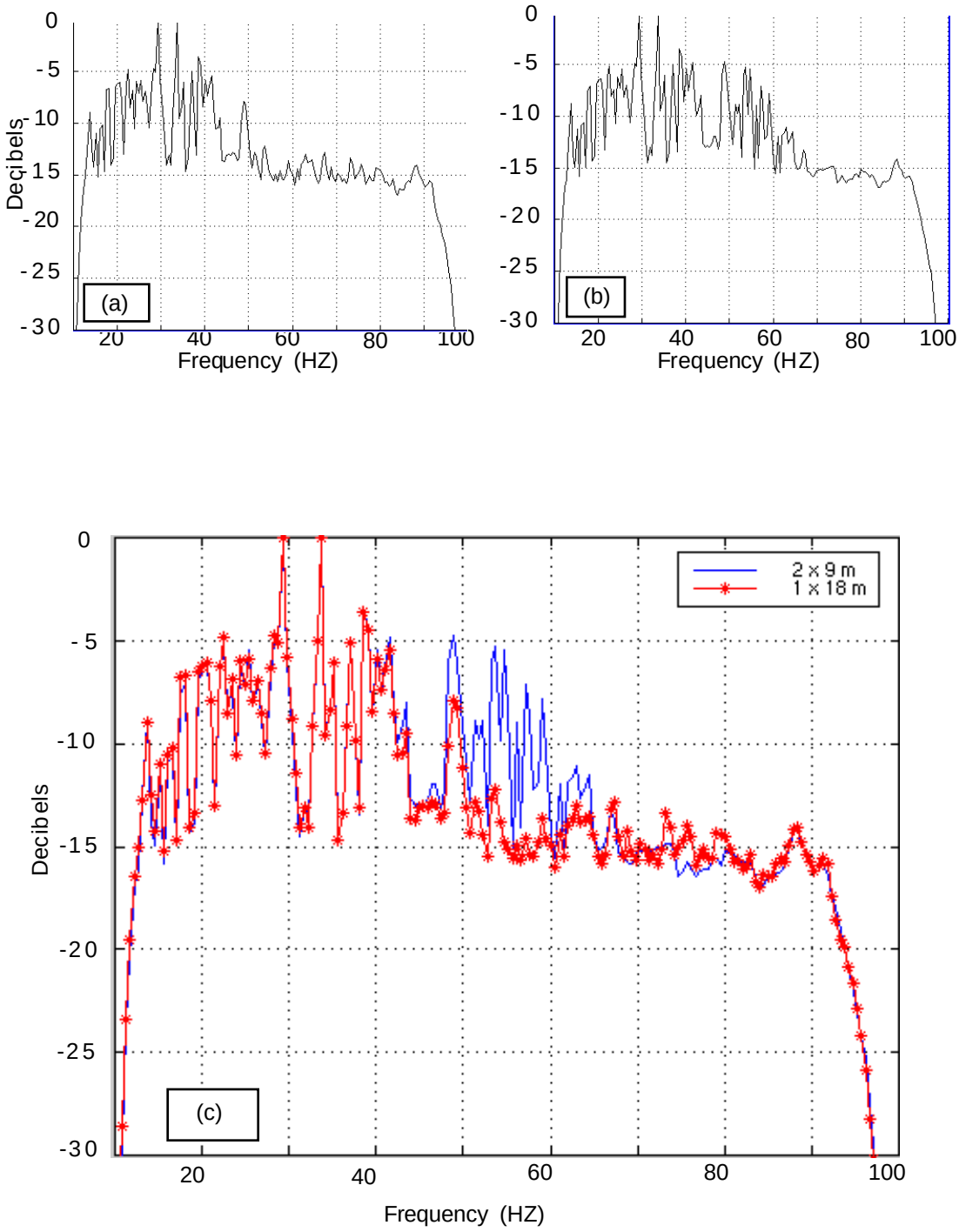

FIGURE 9. Amplitude spectra of the unmigrated prestack TVSW for : (a) 18 m data (b) 9 m data and (c) both spectra were superimposed.

Contents

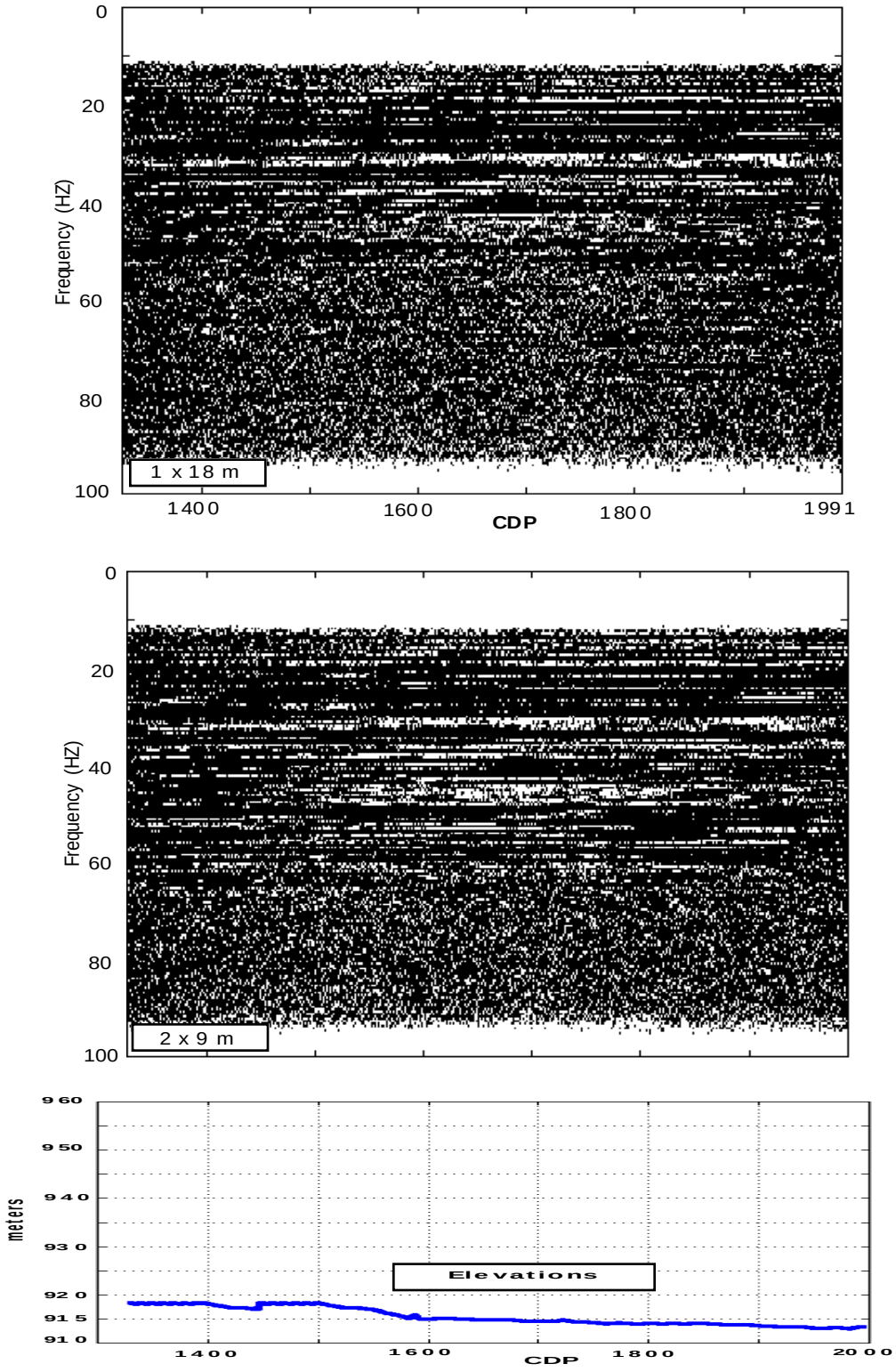

FIGURE 10. The f-x amplitude spectra of the unmigrated poststack TVSW of 18 m and 9 m data and the elevation changes along the processed line.

Contents

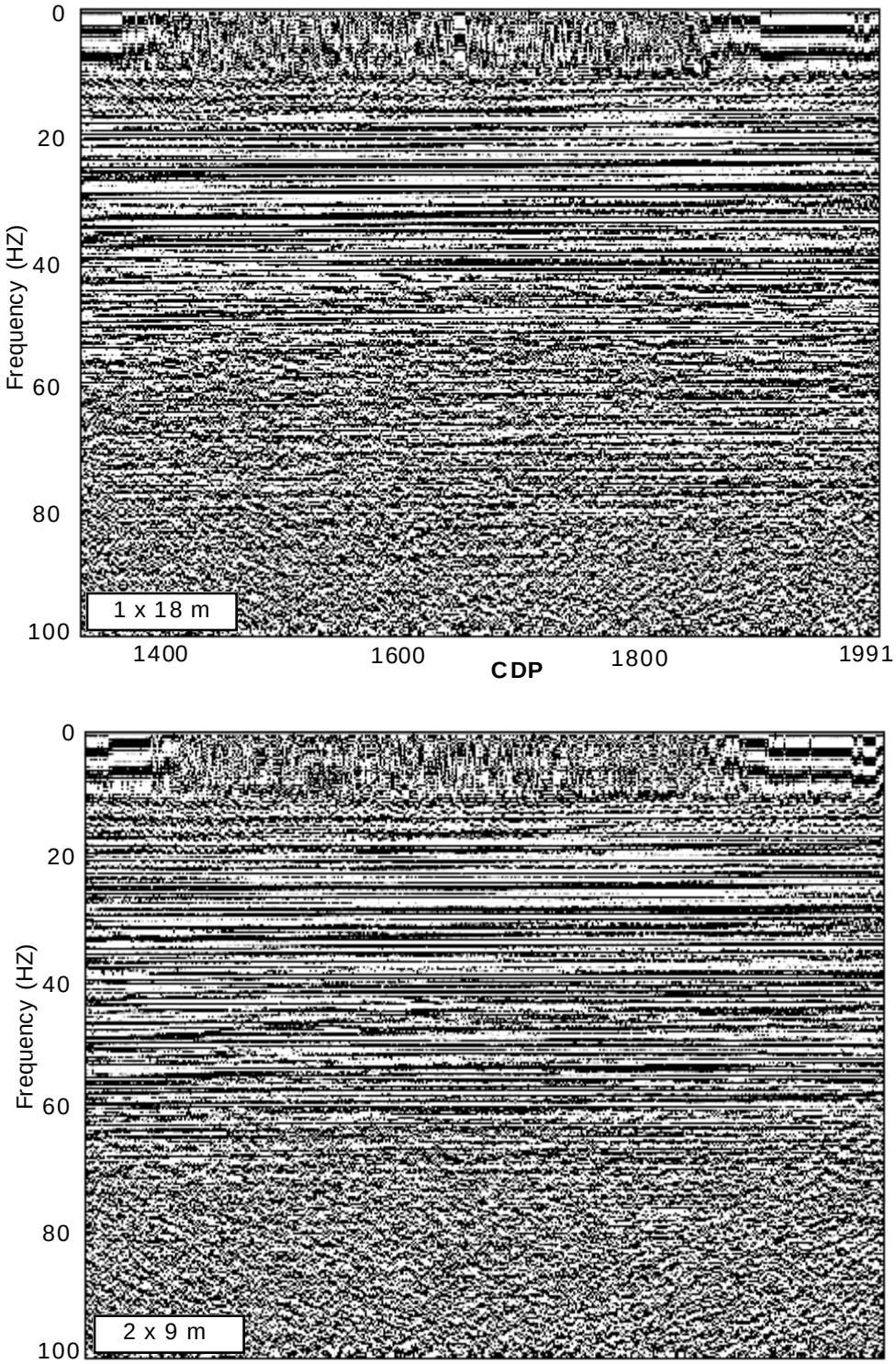

FIGURE 11. The f-x phase spectra of the unmigrated poststack TVSW of the 18 m and 9 m data sets

Contents

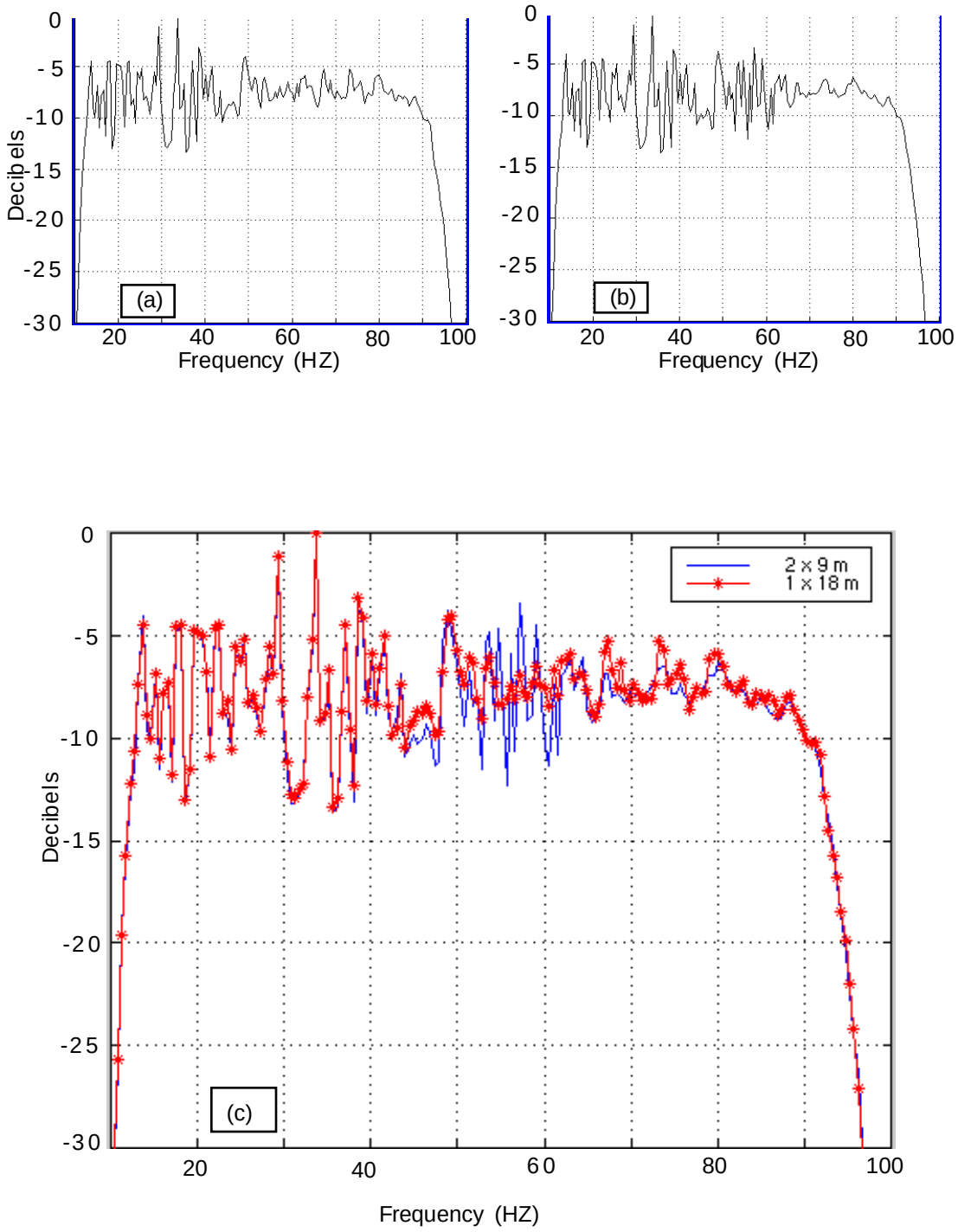

FIGURE 12. The amplitude spectra of the unmigrated poststack TVSW for : (a) 18 m data, (b) 9 m data and (c) both spectra were superimposed.

Contents

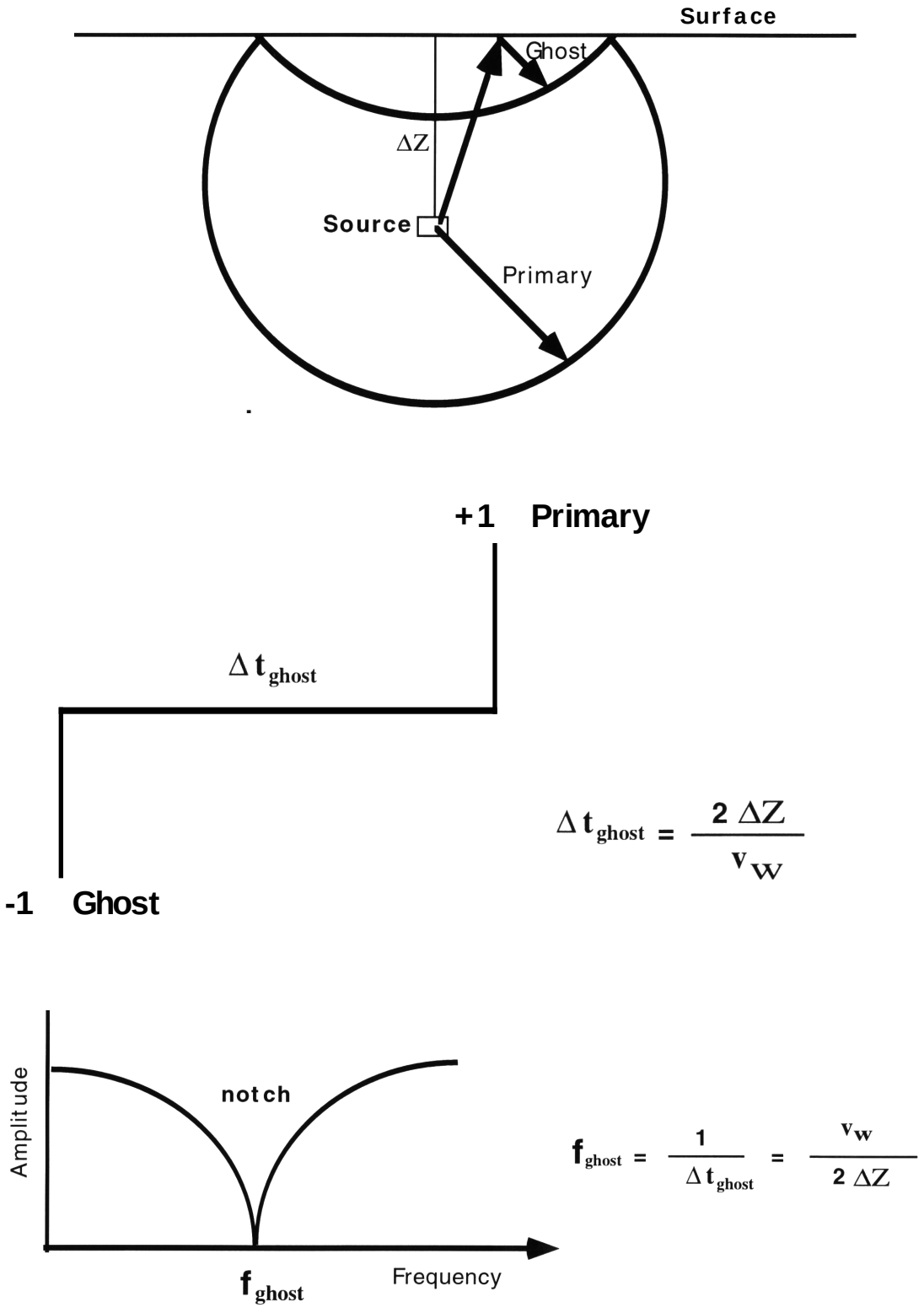

FIGURE 13. A sketch shows a surface ghost from a buried source causes a spectral notch.

Contents

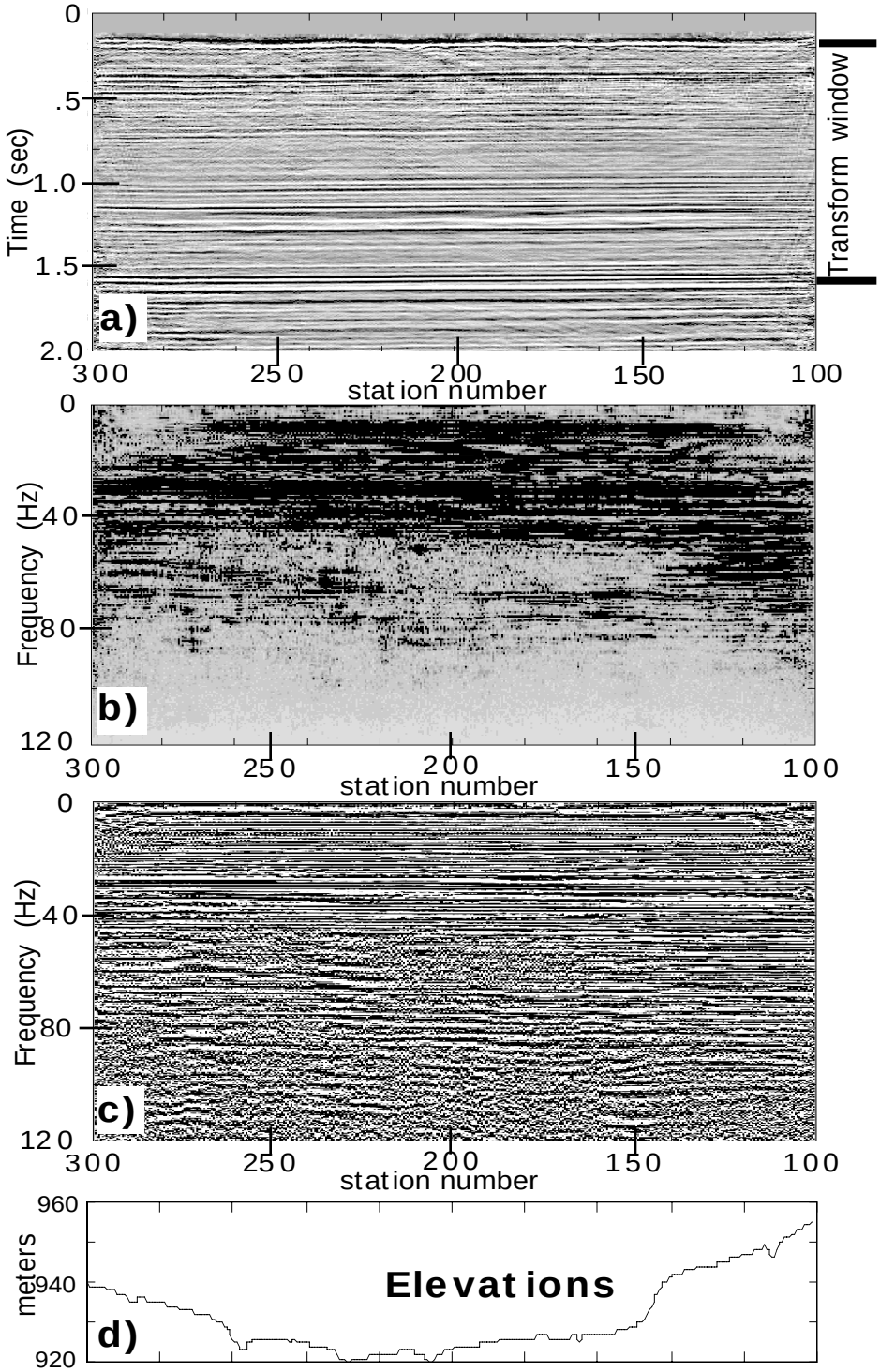

FIGURE 14. The final stack for the Blackfoot 10 HZ array data (a) and its f-x spectral analysis. The amplitude spectrum (b) and the complex phase spectrum (c) were computed over the time zone 0.2 to 1.6 seconds and the elevation along the line. Note the spatial correlation of the spectral notch near 55 HZ. (after Margrave 1995).

Contents

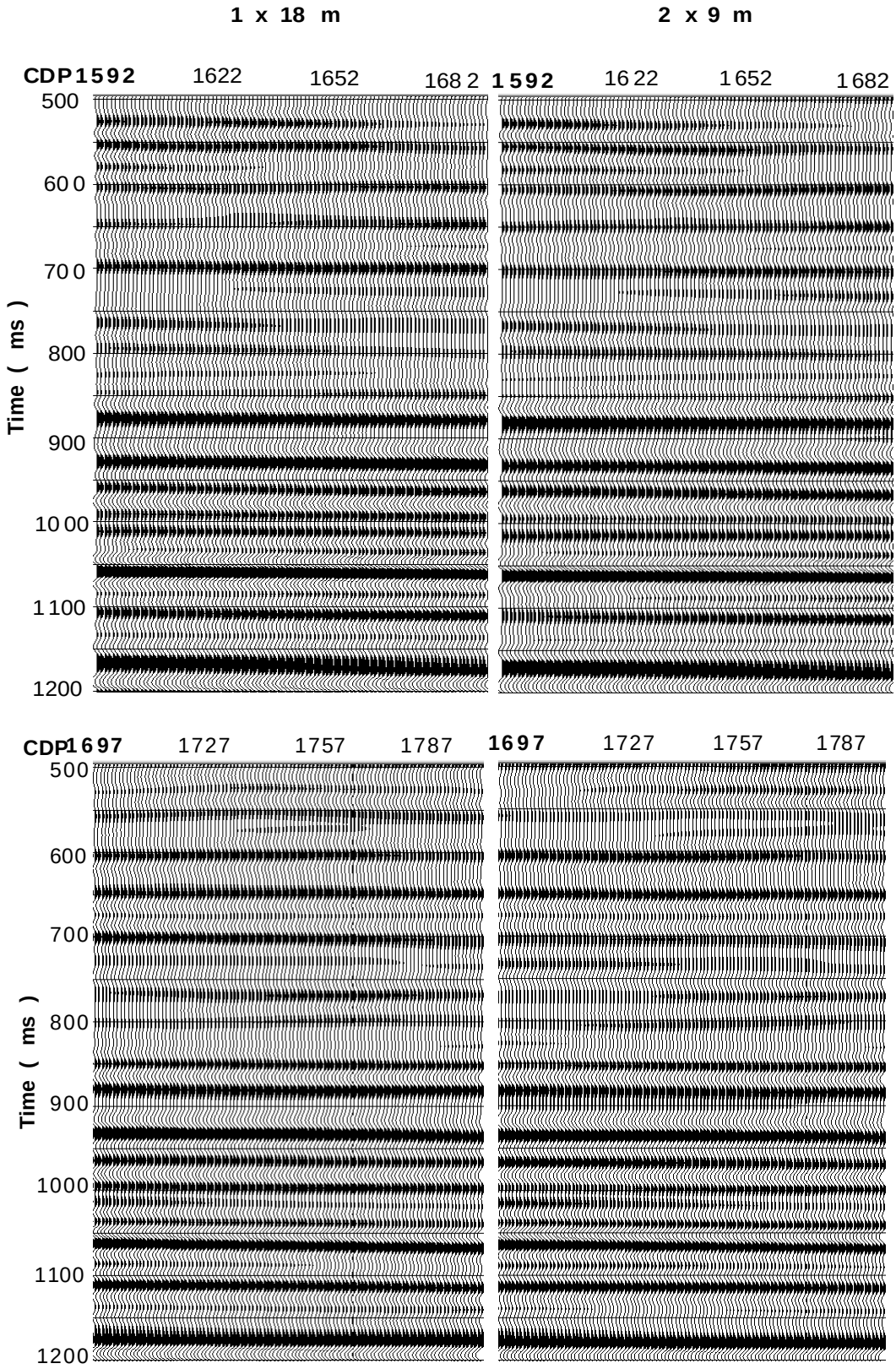

FIGURE 15. Two parts of the selection windows from the migrated and filtered to 50 HZ. of the 18 m and 9 m data in Figure 5. On top are the left halves of the windows while on bottom are the right halves.

Contents

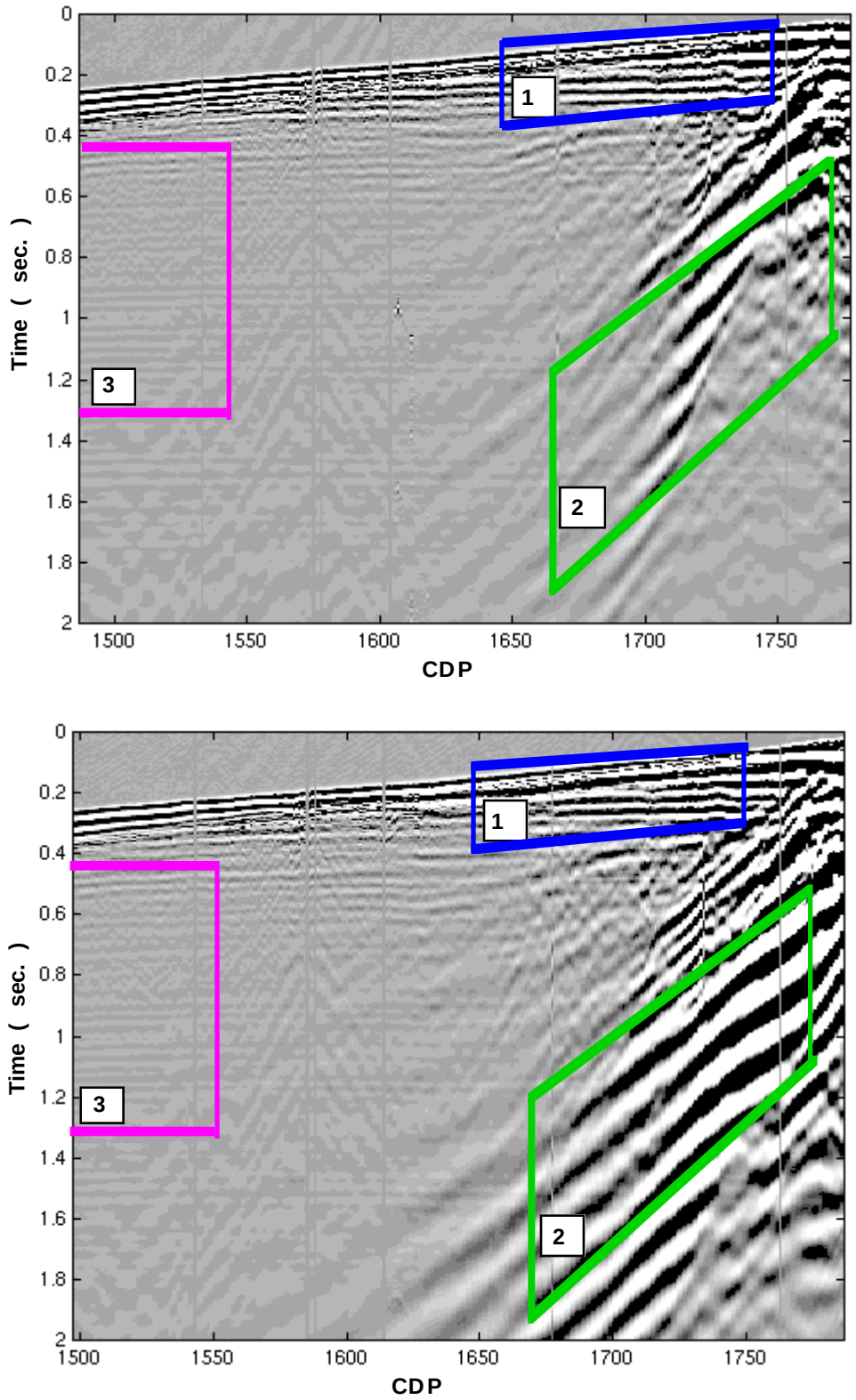

FIGURE 16. Same shot gather for 18 m (top) and 9m (bottom) with selected windows for spectra analysis.

Contents

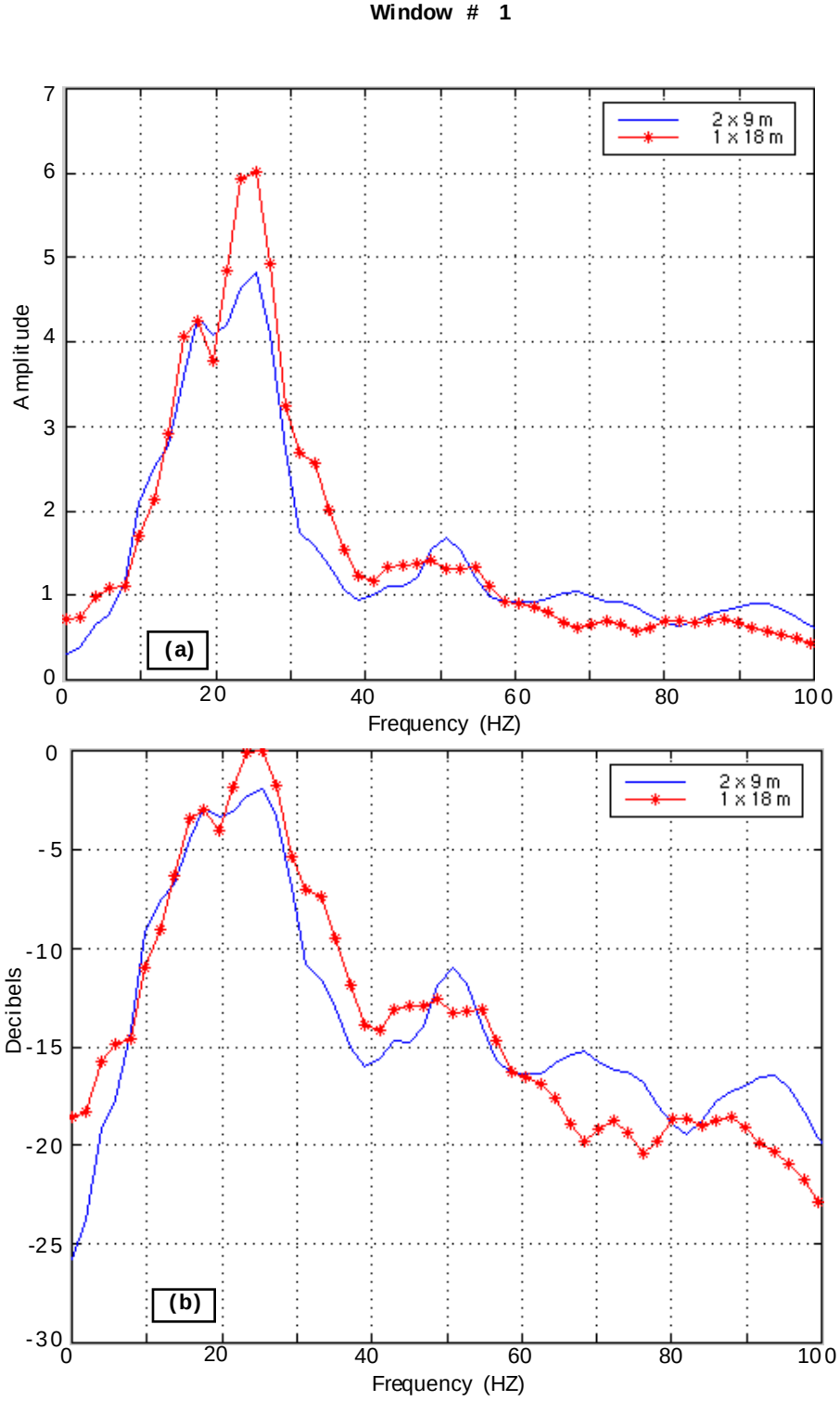

FIGURE 17. Superimposed of (a) the average amplitude spectra of each shot gather and (b) the computed average amplitude spectra with decibel scale with respect to the maximum amplitude of 18 m shot gather.

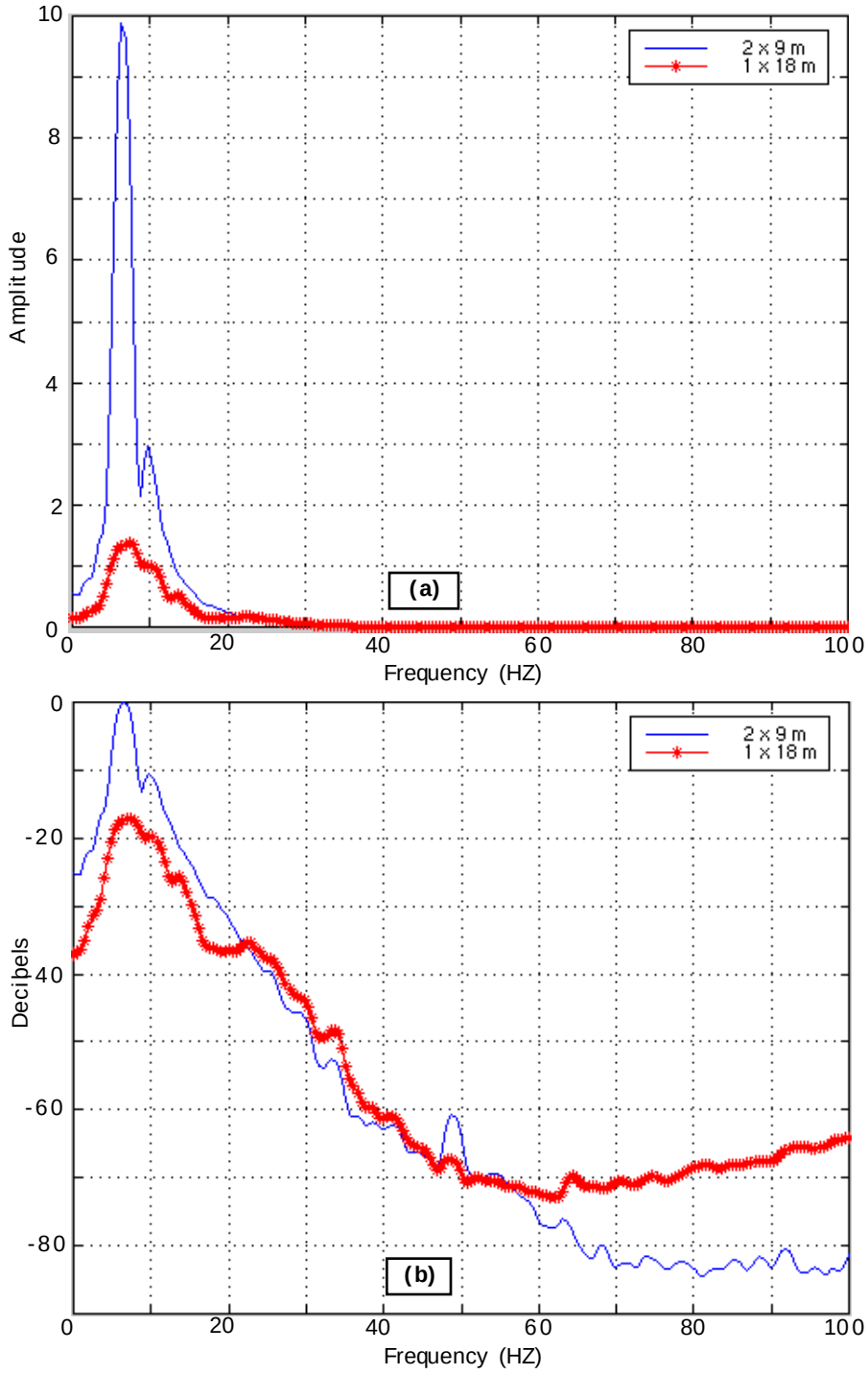

FIGURE 18. Superimposed of (a) the average amplitude spectra of each shot gather and (b) the computed average amplitude spectra with decibel scale with respect to the maximum amplitude of 9 m shot gather.

Contents

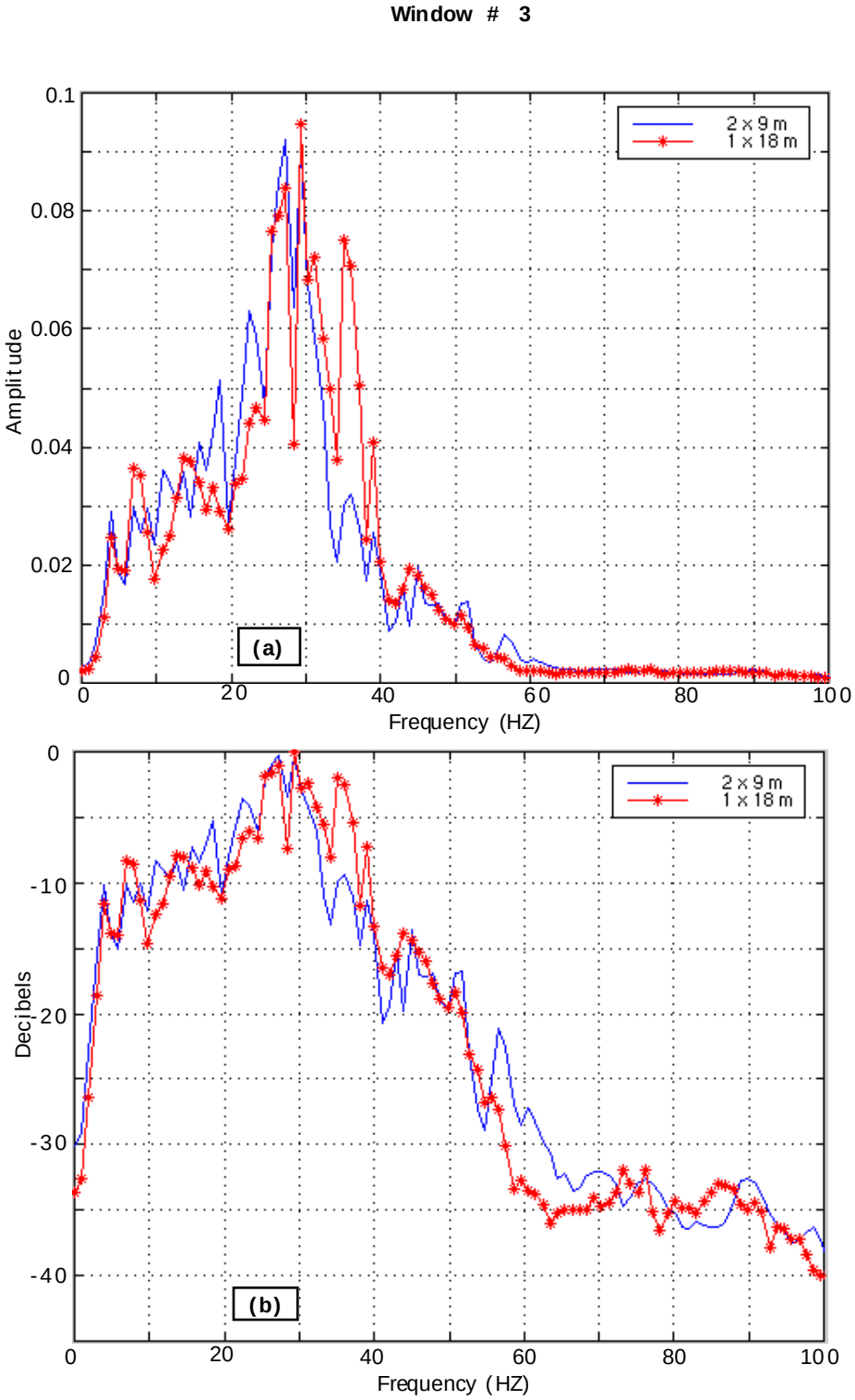

FIGURE 19. Superimposed of (a) the average amplitude spectra of each shot gather and (b) the computed average amplitude spectra with decibel scale with respect to the maximum amplitude of 18 m shot gather.

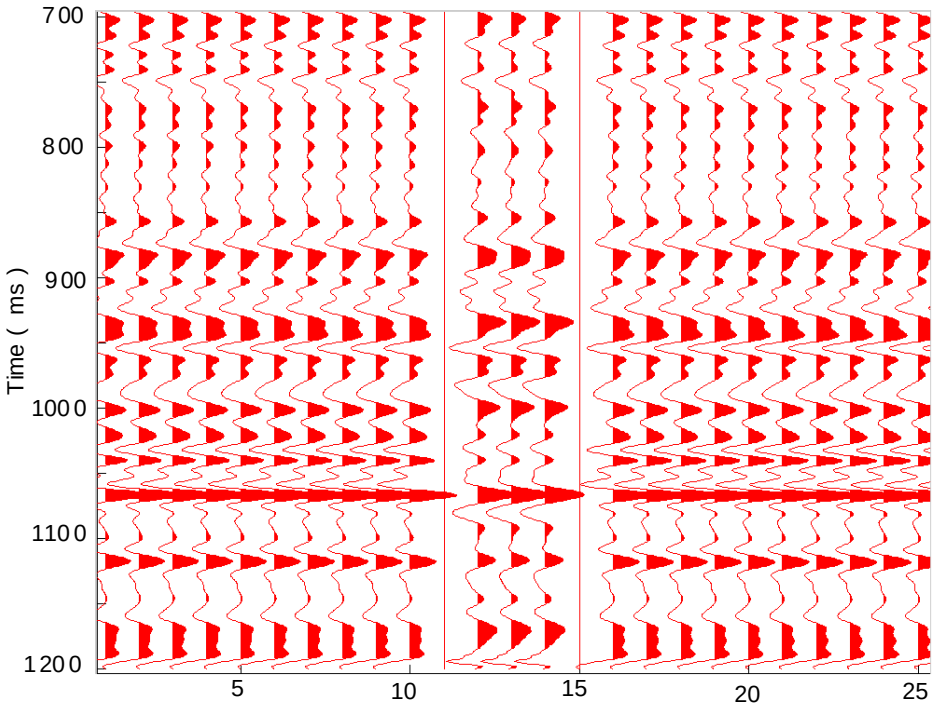

FIGURE 20. A 9m-migrated trace was convolved with a ghost operator (12-14) and some traces from the 18 m migrated stack (1-10,16-25).

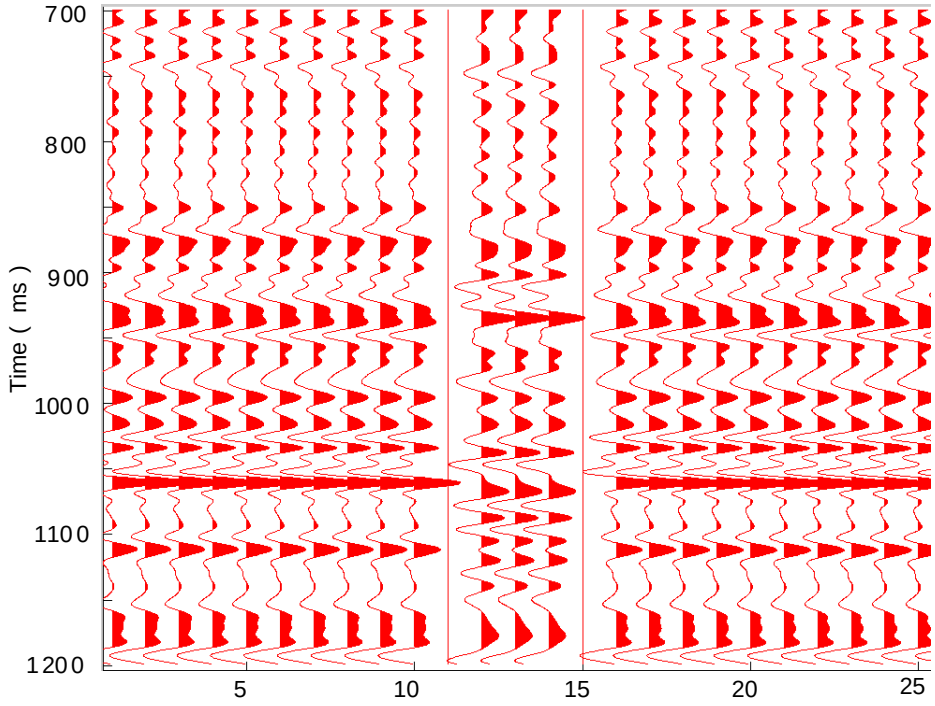

FIGURE 21. A 9m-migrated trace (12-14) and some traces from the 18 m migrated stack (1-10,16-25).

Contents